Electronic Supplementary Material (ESI) for Journal of Materials Chemistry A.

Electronic Supporting Information

IrRu alloy nanocactus on a $Cu_{2-x}S@IrS_y$ core as a highly efficient bifunctional electrocatalyst toward overall water splitting in acidic electrolyte

Jinwhan Joo, †[ab] Haneul Jin, †[ab] Aram Oh,[c] Byeongyoon Kim [ab], Jaeyoung Lee,[b] Hionsuck Baik,[c] Sang Hoon Joo,[de] and Kwangyeol Lee*[ab]

a. Center for Molecular Spectroscopy and Dynamics, Institute for Basic Science (IBS), Seoul 02841, Republic of Korea.

b. Department of Chemistry, Korea University, Seoul 02841, Republic of Korea.

c. Korea Basic Science Institute (KBSI), Seoul 02841, Republic of Korea.

d. School of Energy and Chemical Engineering, Ulsan National Institute of Science and Technology (UNIST), Ulsan 44919, Republic of Korea.

† These authors contributed equally.

* Corresponding author: Kwangyeol Lee, E-mail: kylee1@korea.ac.kr

1. Supporting Figures S1 to S20

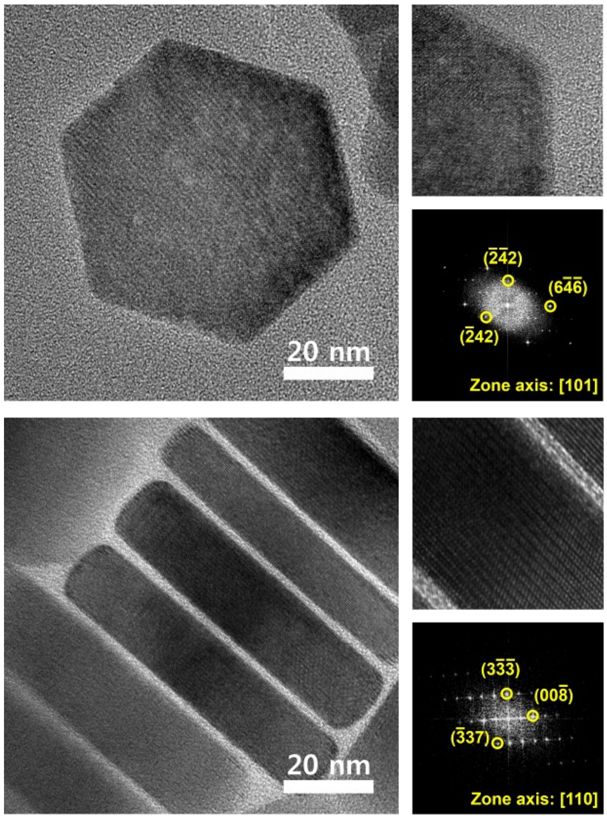

Fig. S1. HRTEM images and corresponding FFT patterns of $Cu_{2-x}S@IrS_y$

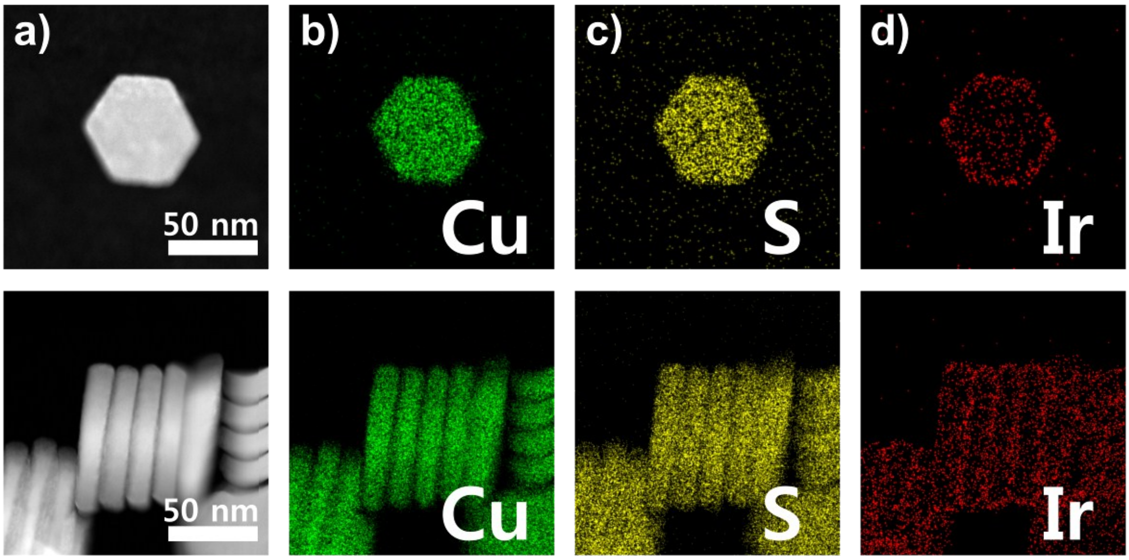

Fig. S2. Scaning Transmission electron microscopy (STEM) and elemental mapping analysis of CIS template. a) STEM image of CIS template, b) Cu (green), c) S (yellow), d) Ir (red).

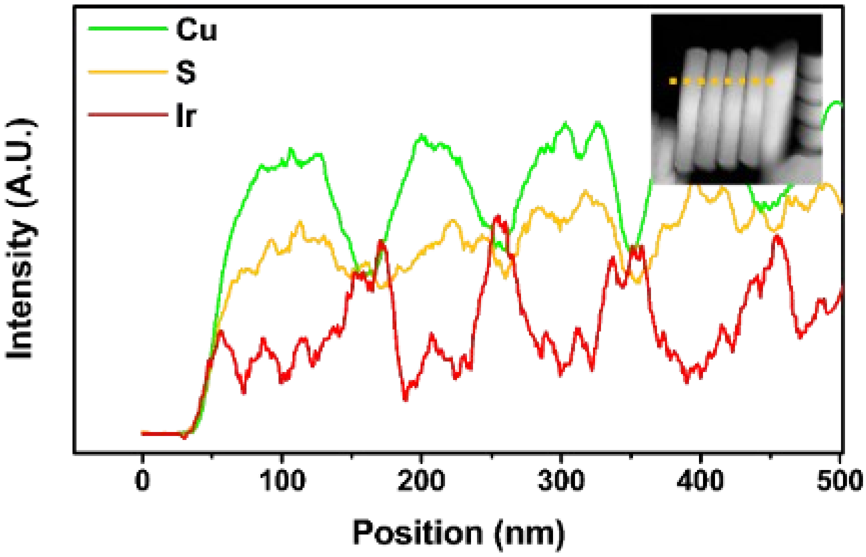

Fig. S3. Compositional line profile of CIS template. The inset of STEM image indicate line scan direction for the corresponding nanoparticles.

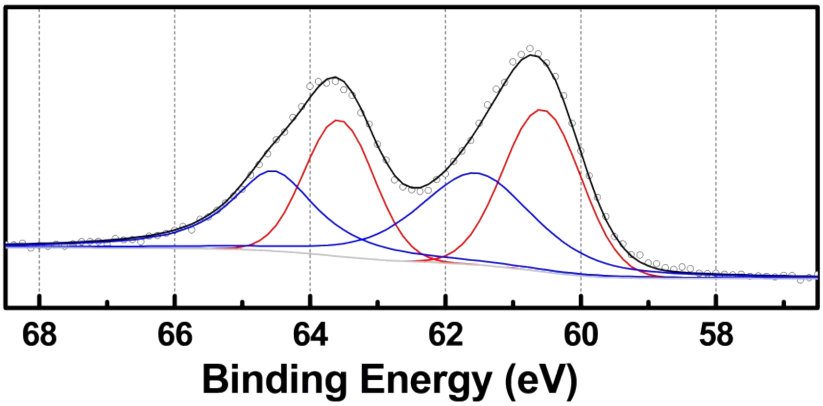

Fig. S4. XPS analysis of Ir 4f in CIS template. Each colour indicates metallic Ir (red) and oxidized Ir (blue)

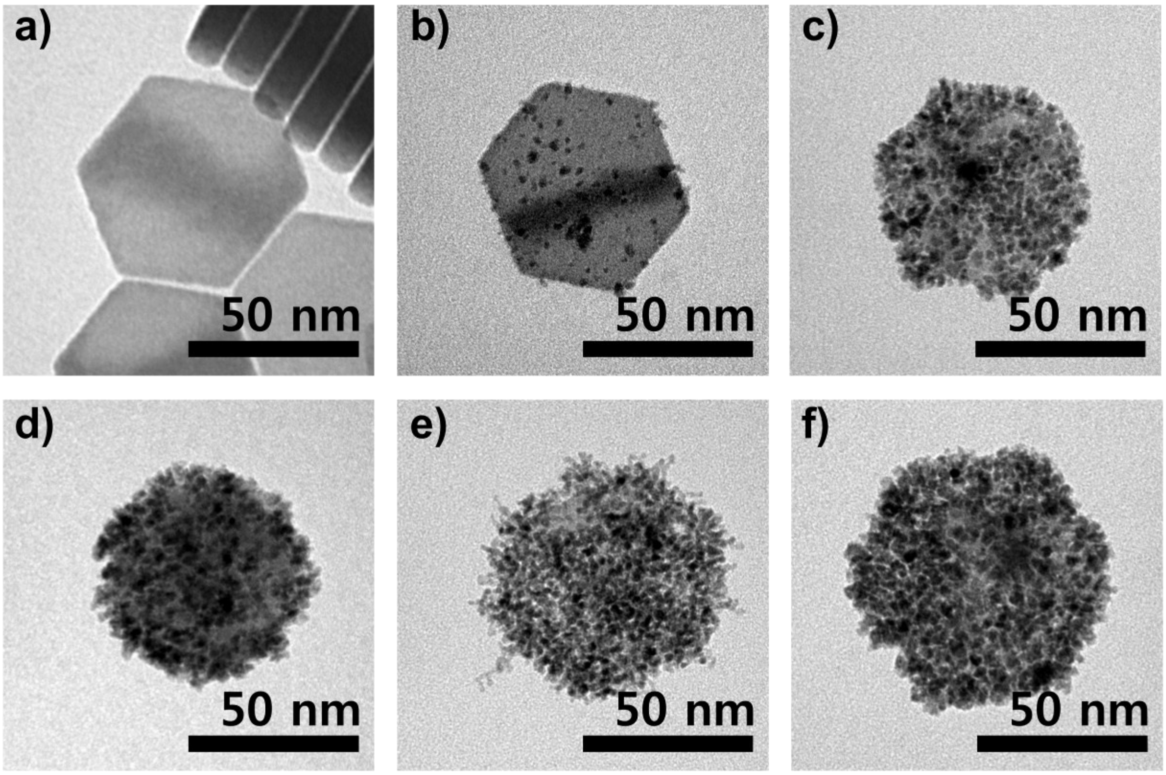

Fig. S5. TEM images of temporal reaction intermediates. a) template, b) 4 min, c) 8 min, d) 16 min, e) 30 min, and f) 60 min.

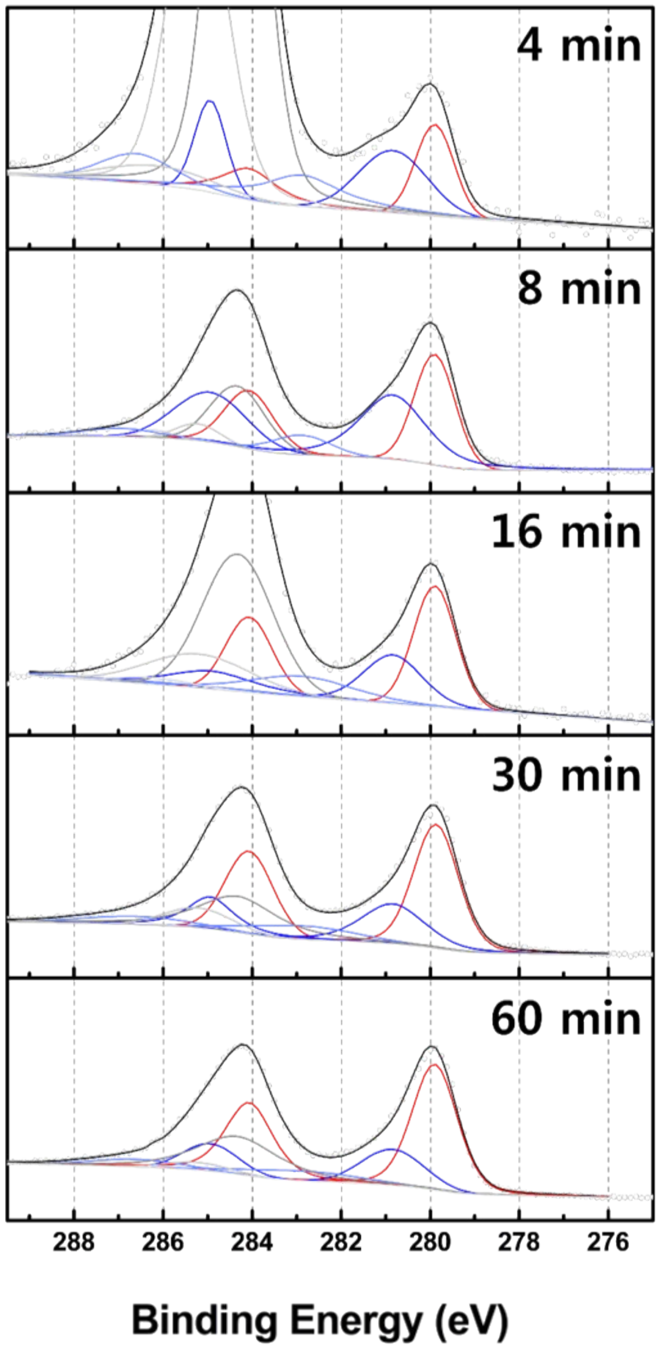

Fig. S6. XPS analysis of Ru on CIS@$Ir_{48}Ru_{52}$ for reaction intermediates at 4 min, 8 min, 16 min, 30 min, and 60 min. Each colour indicates metallic Ru (red), oxidized Ru (blue and pastel blue), and carbon (grey colour).

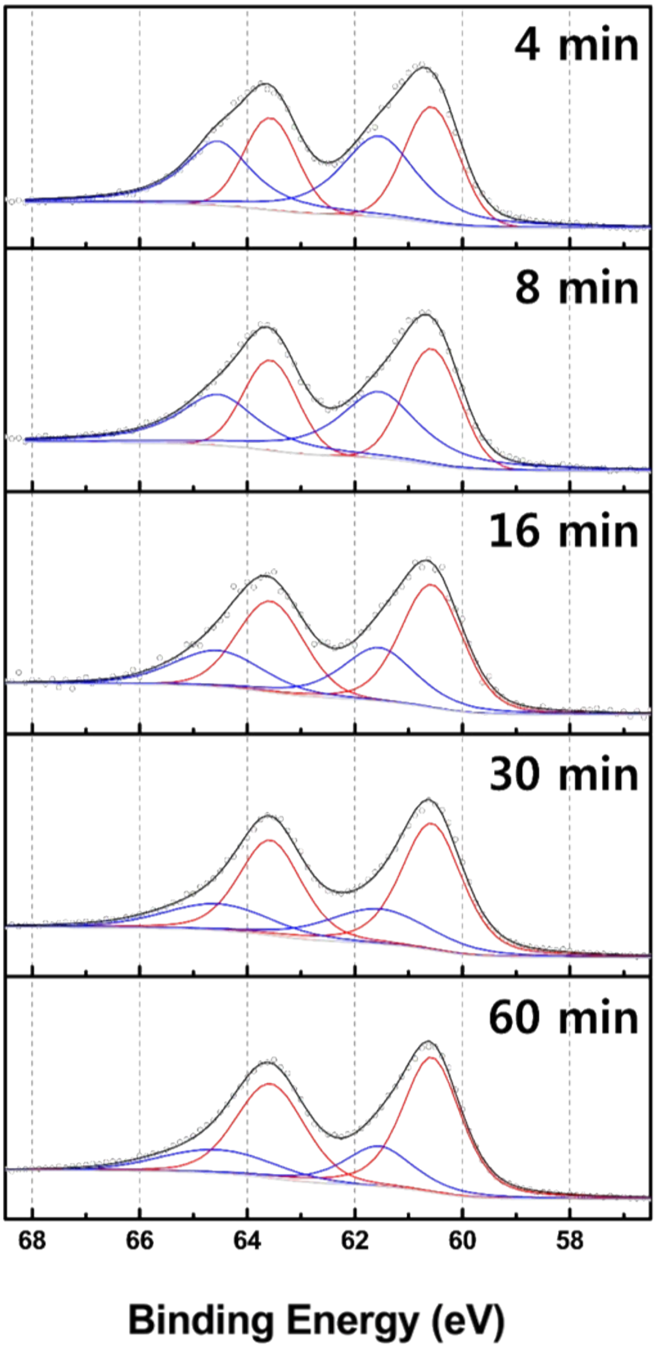

Fig. S7. XPS analysis of Ir 4f on CIS@$Ir_{48}Ru_{52}$ for reaction intermediates at 4 min, 8 min, 16 min, 30 min, and 60 min. Each colour indicates metallic Ir (red) and oxidized Ir (blue).

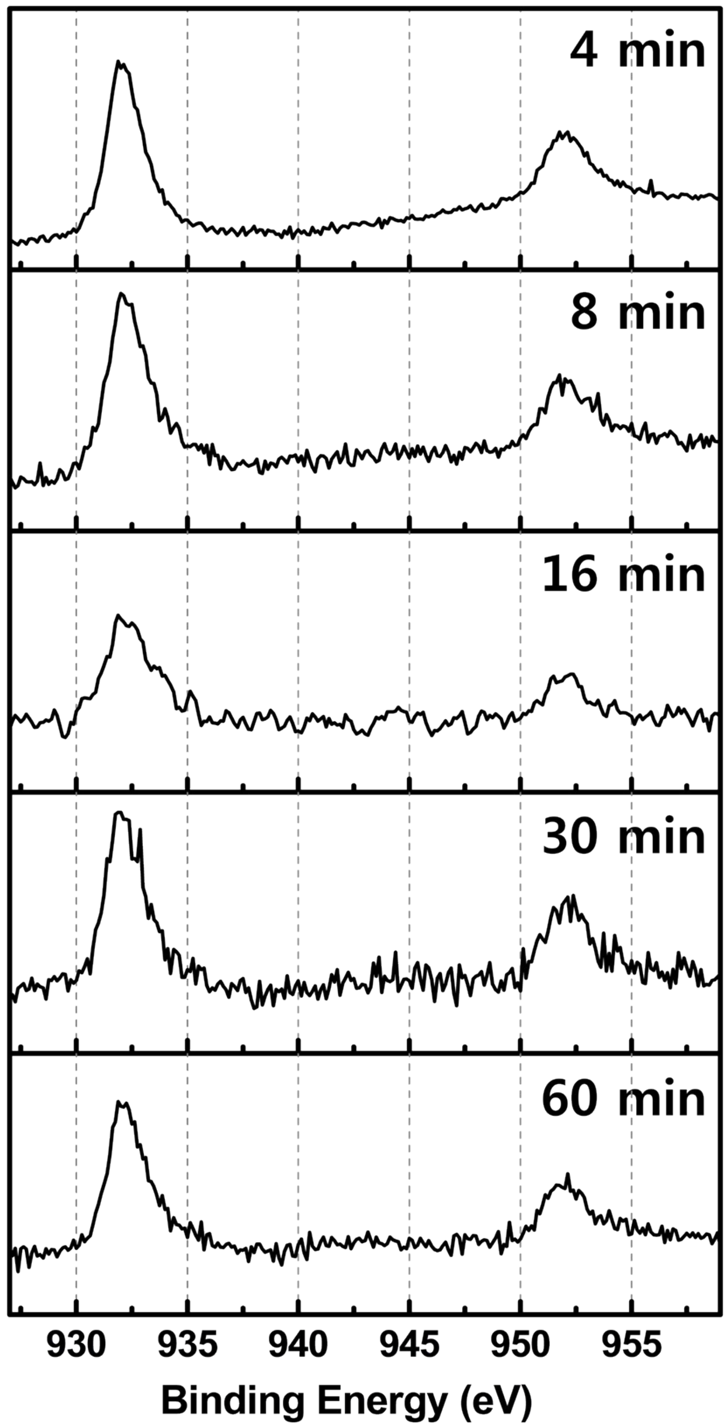

Fig. S8. XPS analysis of Cu 2p on CIS@$Ir_{48}Ru_{52}$ for reaction intermediates at 4 min, 8 min, 16 min, 30 min, and 60 min.

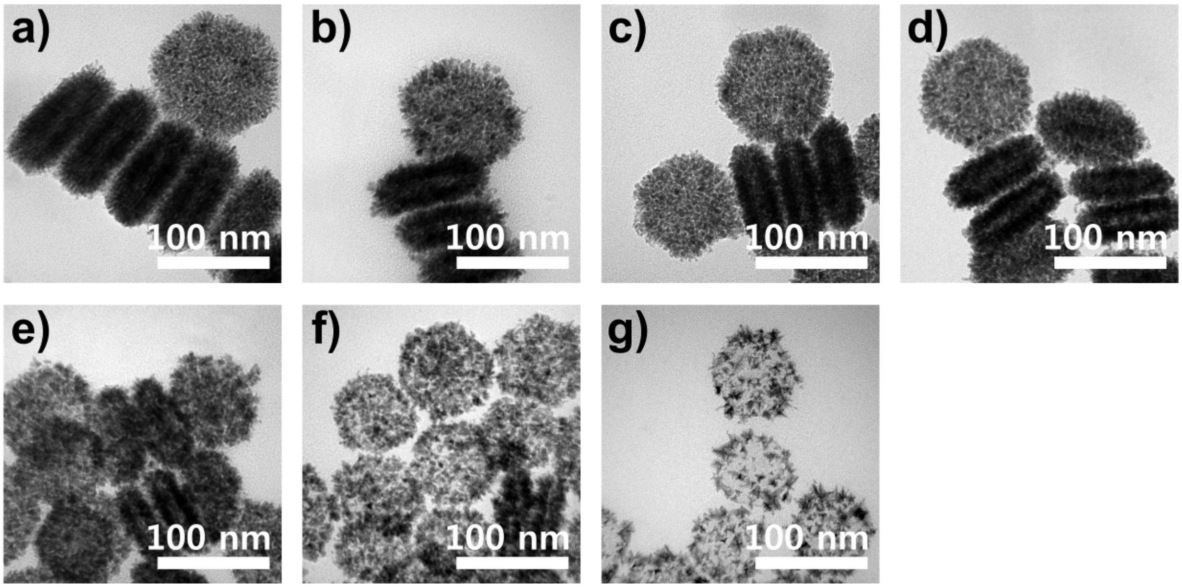

Fig. S9. TEM images of CIS@Ir_xRu_{1-x} with various ratio of Ir to Ru precursors at second reaction step. The ratio of Ir to Ru is a) 1:0, b) 5:1, c) 2:1, d) 1:1, e) 1:2, f) 1:5, and g) 0:1, respectively.

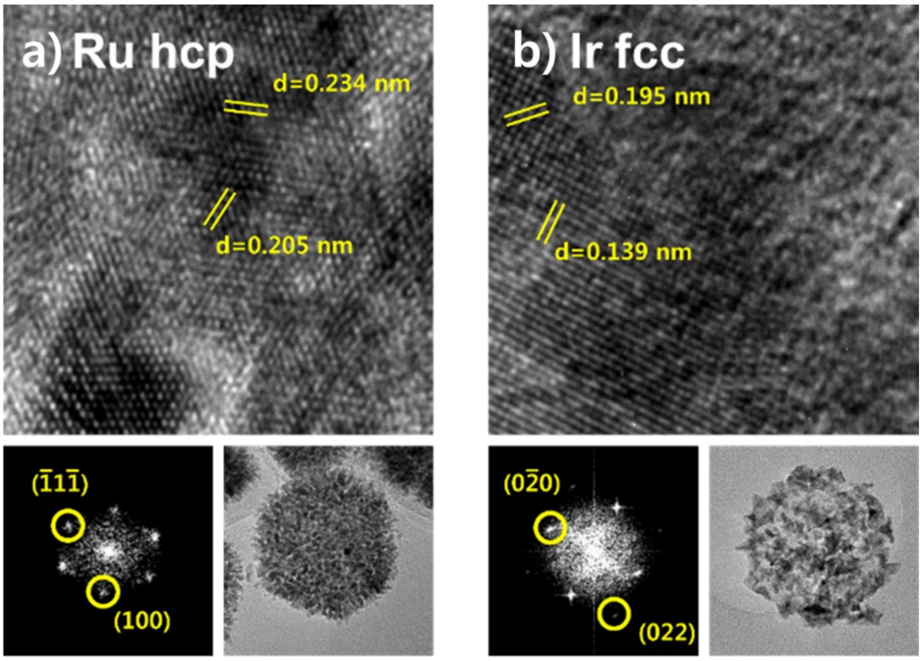

Fig. S10. HRTEM images of CIS@Ir_xRu_{1-x} with various ratio of Ir to Ru precursors at second reaction step. The ratio of Ir to Ru is a) 1:0, and b) 0:1, respectively

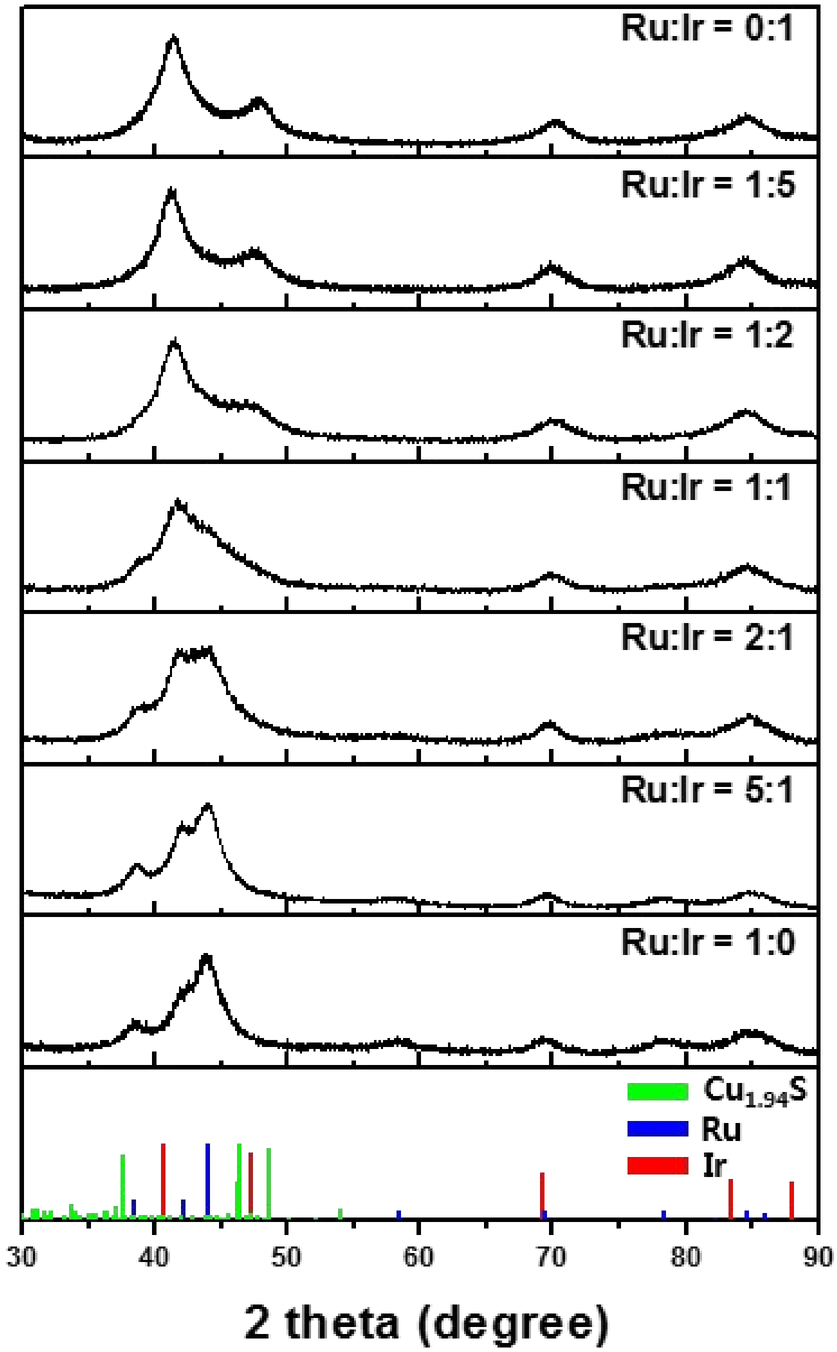

Fig. S11. XRD patterns of CIS@Ir_xRu_{1-x} with various ratio of Ir to Ru precursors at second reaction step. The colour sticks indicate the reference X-ray diffraction lines: red, Ir (JCPDS # 06-0598), blue, Ru (JCPDS # 70-0274), and green, $Cu_{1.94}S$ (JCPDS # 34-0660).

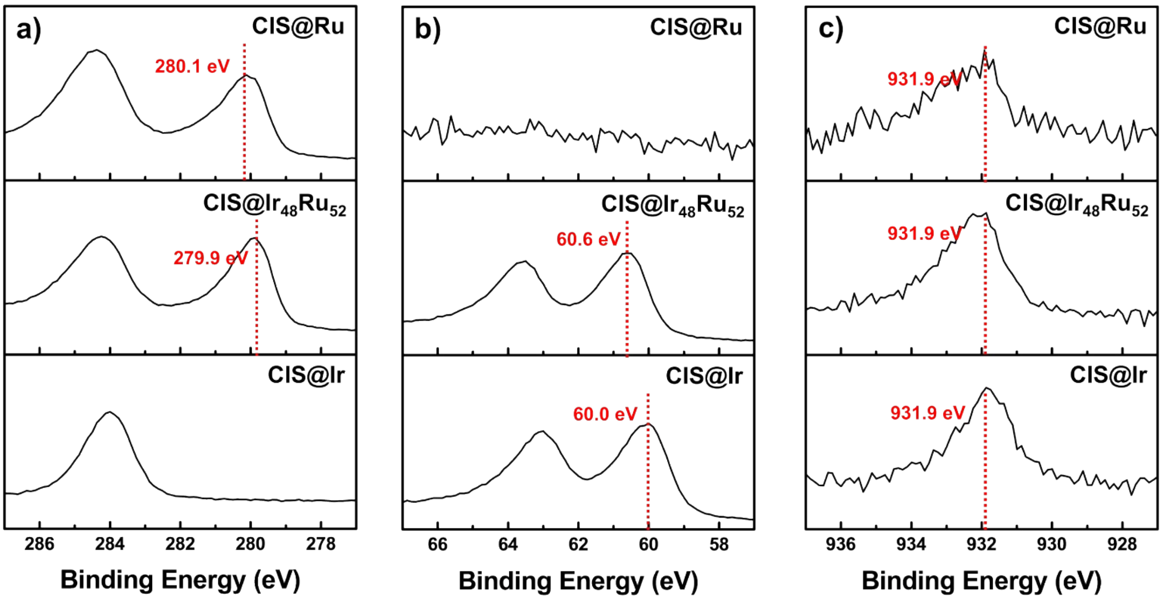

Fig. S12. XPS analysis of a) Ru 3d, b) Ir 4f, and c) Cu 2p in CIS@Ru, CIS@$Ir_{48}Ru_{52}$, and CIS@Ir.

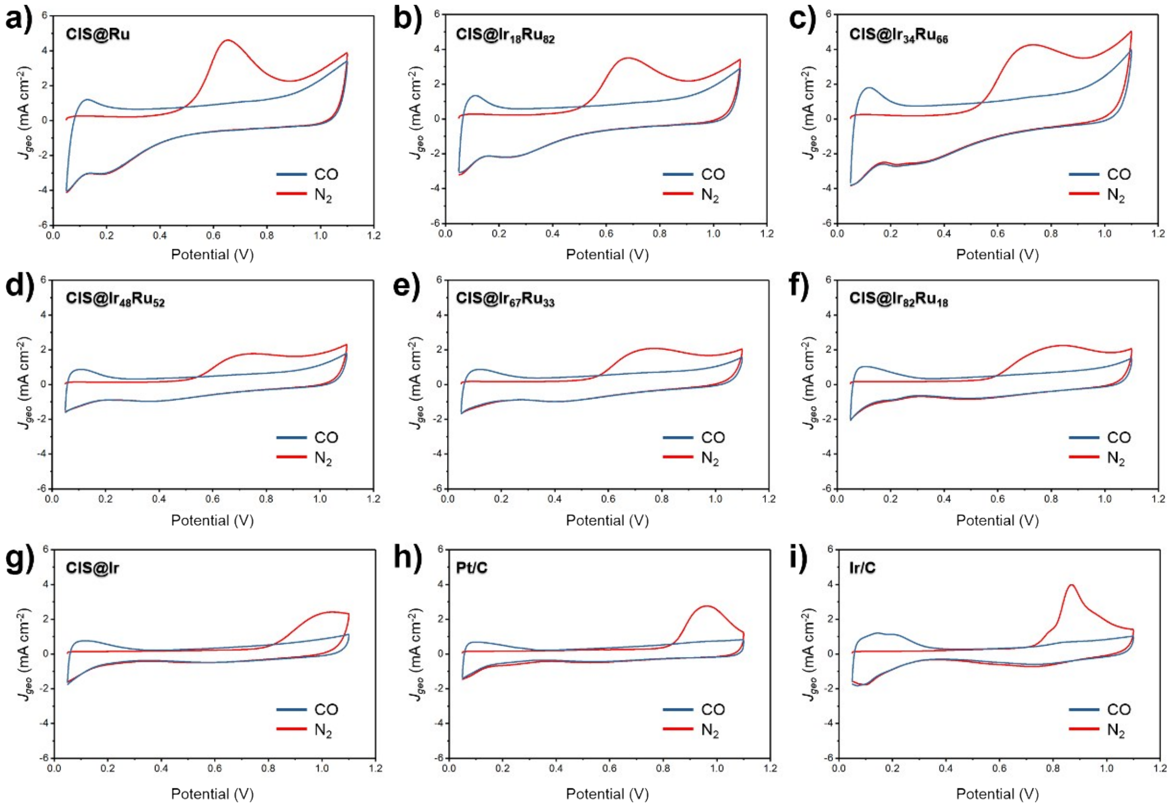

s

Fig. S13. CO stripping measurements of a) CIS@Ru, b) CIS@$Ir_{18}Ru_{82}$, c) CIS@$Ir_{34}Ru_{66}$, d) CIS@$Ir_{48}Ru_{52}$, e) CIS@$Ir_{67}Ru_{33}$, f) CIS@$Ir_{82}Ru_{18}$, g) CIS@Ir, h) Pt/C, and i) Ir/C in N_2-saturated electrolyte. Red and blue curves indicate measurement with CO and N_2, respectively.

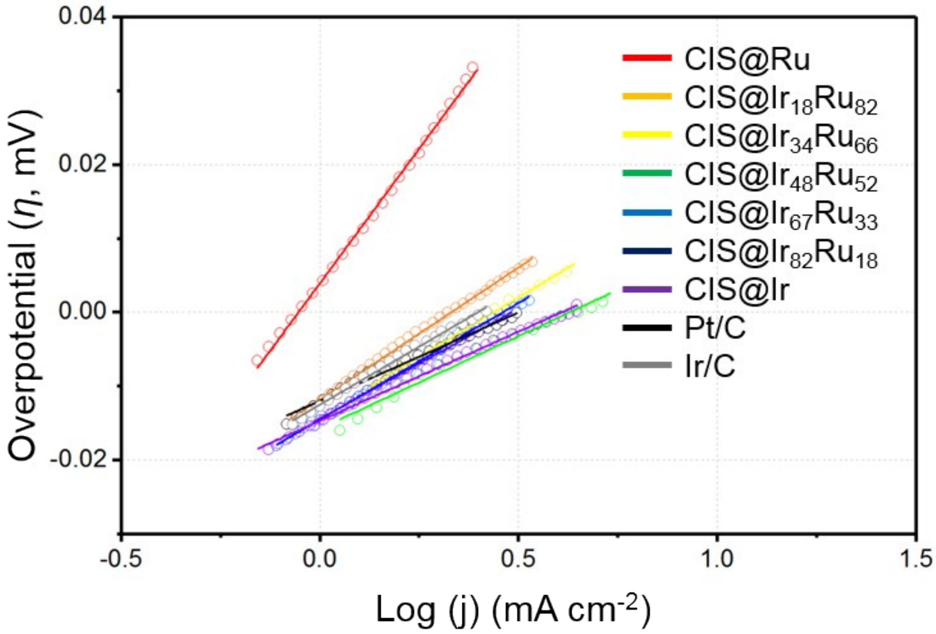

Fig. S14. Tafel plots of various CIS@Ir_xRu_{1-x}, commercial Pt/C, and commercial Ir/C for HER.

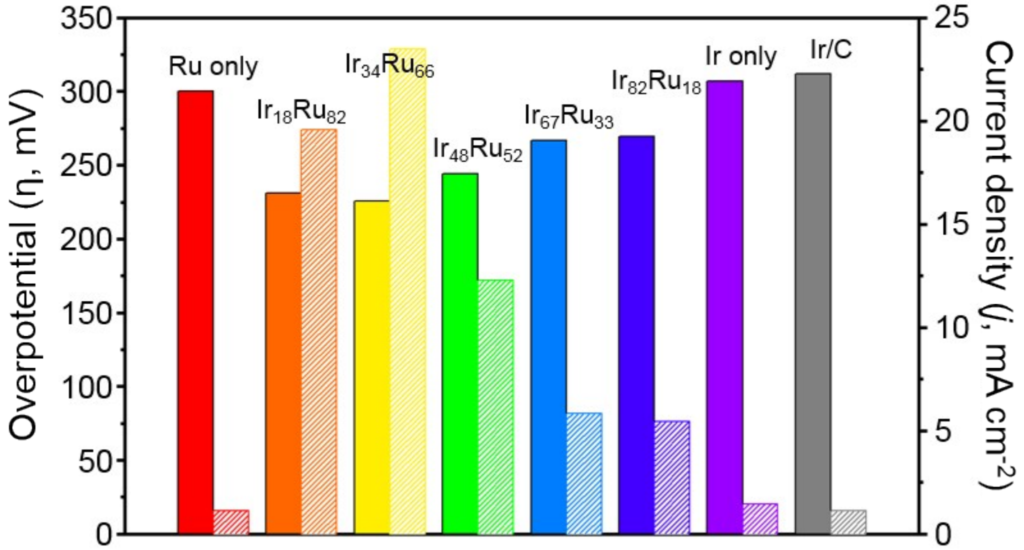

Fig. S15. Comparison of OER activities; plane column for overpotential (η) at 10 mA cm^{-2} (left) and dashed column for current density (*j*) at 1.48 V (right).

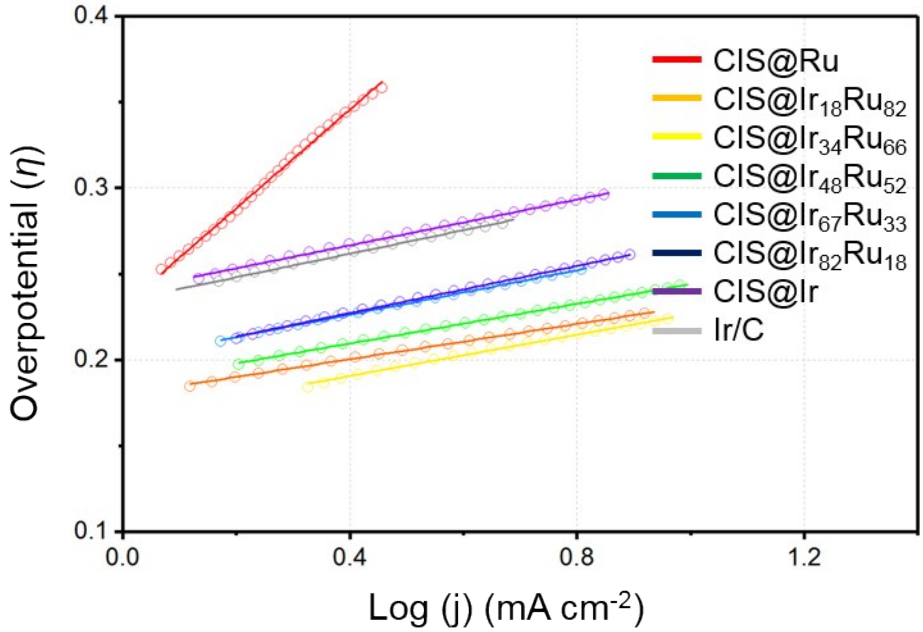

Fig. S16. Tafel plots of various CIS@Ir_xRu_{1-x} and commercial Ir/C for OER.

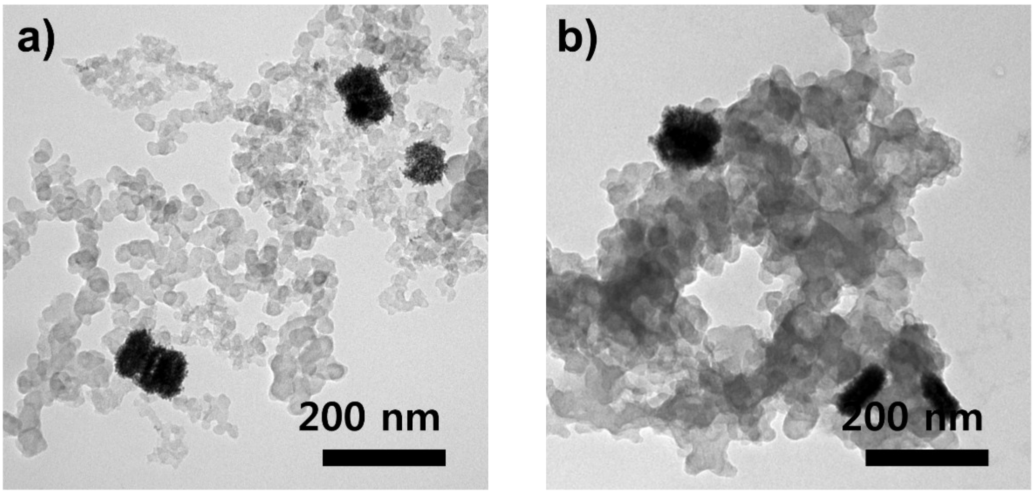

Fig. S17. TEM images of CIS@$Ir_{48}Ru_{52}$ (a) before and (b) after OER stability test. Cactus-like morphology remains after stability test, indicating CIS@$Ir_{48}Ru_{52}$ has robust structure.

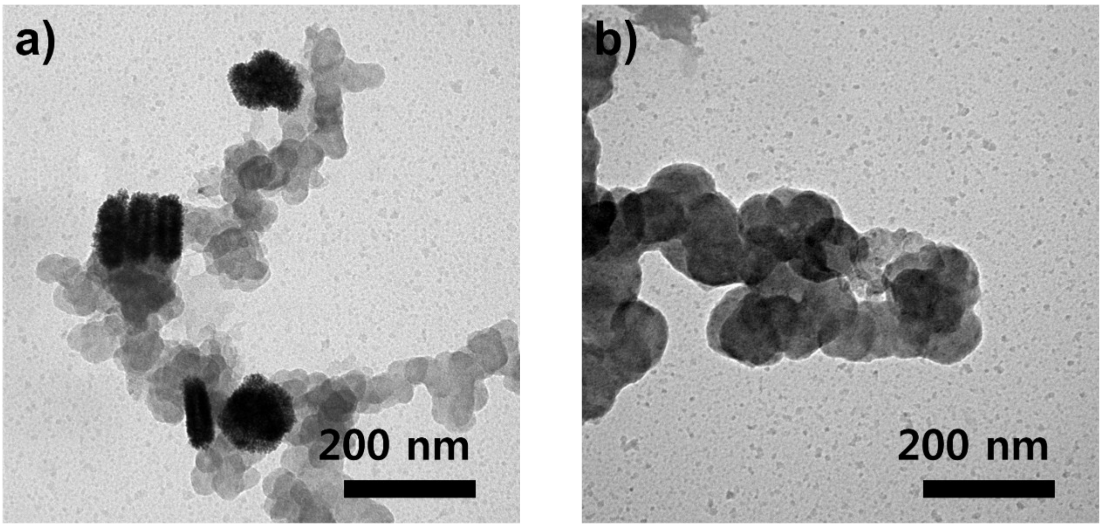

Fig. S18. TEM images of CIS@$Ir_{34}Ru_{66}$ (a) before and (b) after OER stability test.

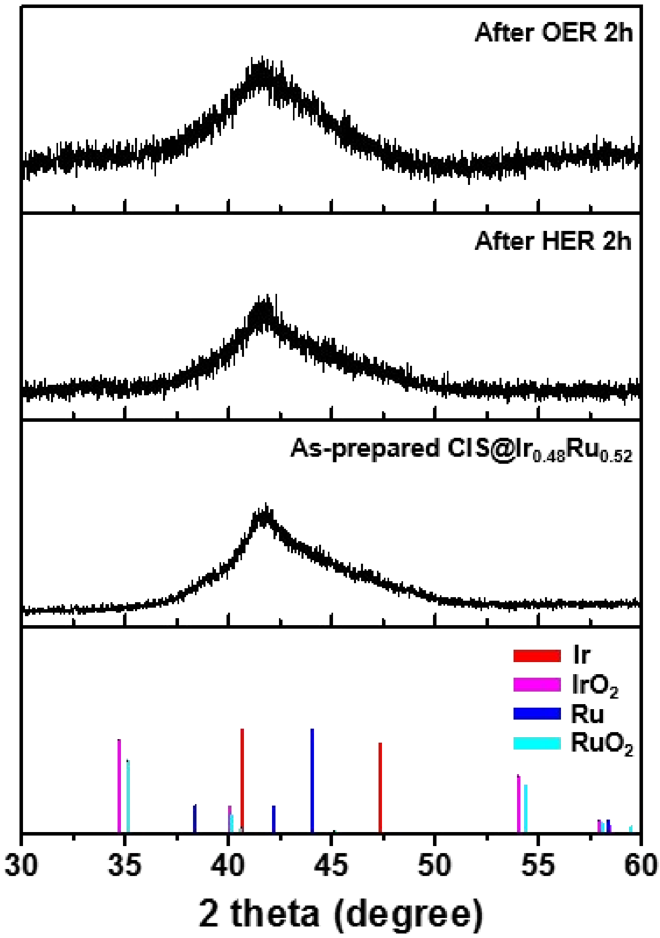

Fig. S19. XRD analysis of CIS@$Ir_{48}Ru_{52}$ after HER (-0.09 V) and OER (1.55 V) at certain potential for 2 h. The colour sticks indicate the reference X-ray diffraction lines: red, (Ir, JCPDS # 06-0598), magenta (IrO_2, JCPDS # 15-0870), blue (Ru, JCPDS # 70-0274), and cyan (RuO_2, JCPDS # 70-2662).

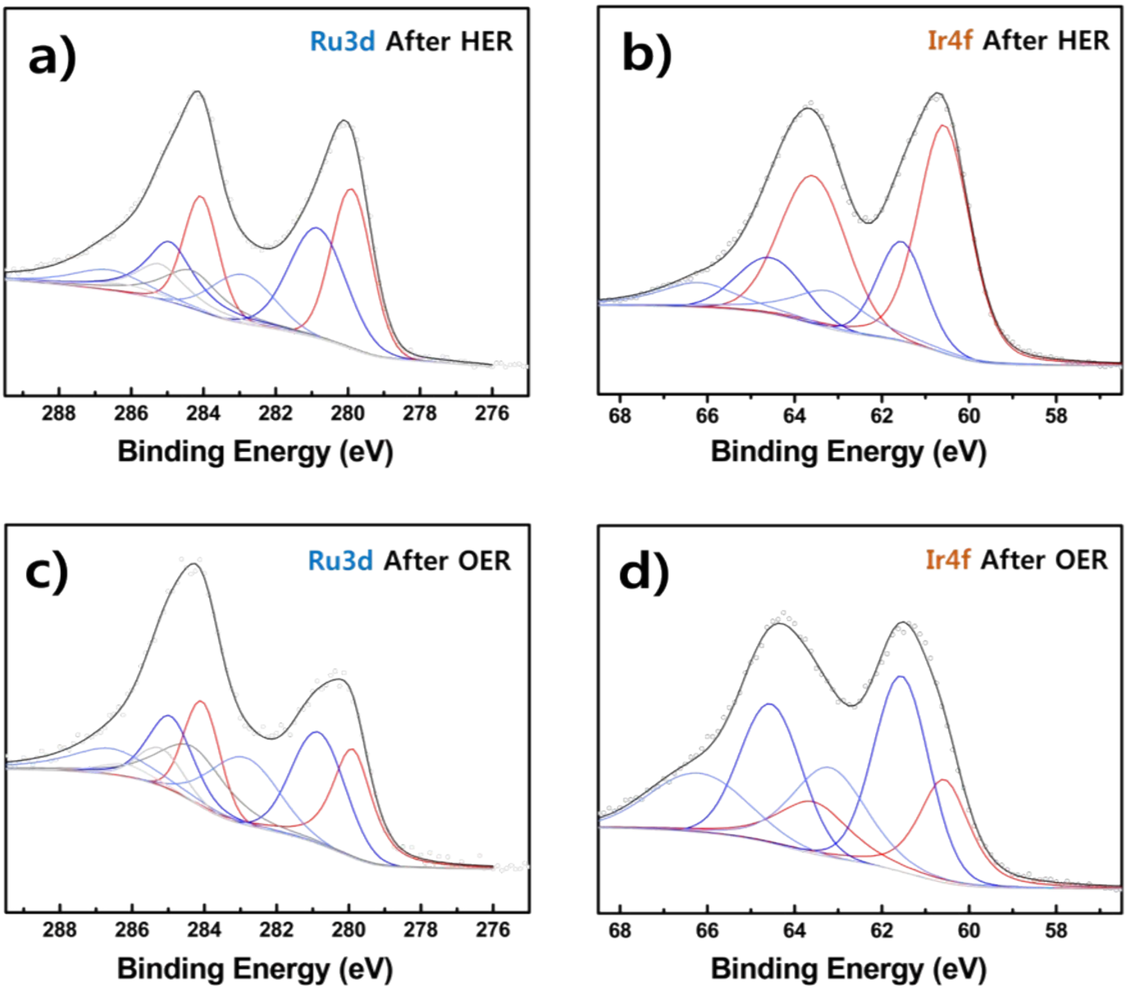

Fig. S20. XPS analysis of Ru 3d and Ir 4f in CIS@$Ir_{48}Ru_{52}$ after HER (-0.09 V) and OER (1.55 V) at certain potential for 2 h. Each colour indicates metallic Ru and Ir (red), oxidized Ru and Ir (blue and pastel blue), and carbon (grey colour). a) Ru3d after HER, b) Ir4f after HER, c) Ru3d after OER, and d) Ir4f after OER

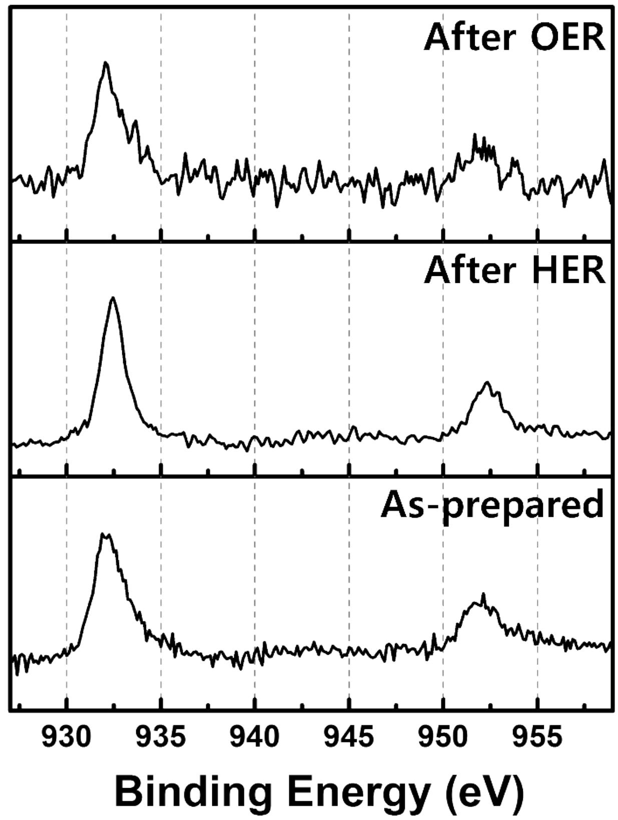

Fig. S21. XPS analysis of Cu 2p in CIS@$Ir_{48}Ru_{52}$ after HER (-0.09 V) and OER (1.55 V) at certain potential for 2 h.

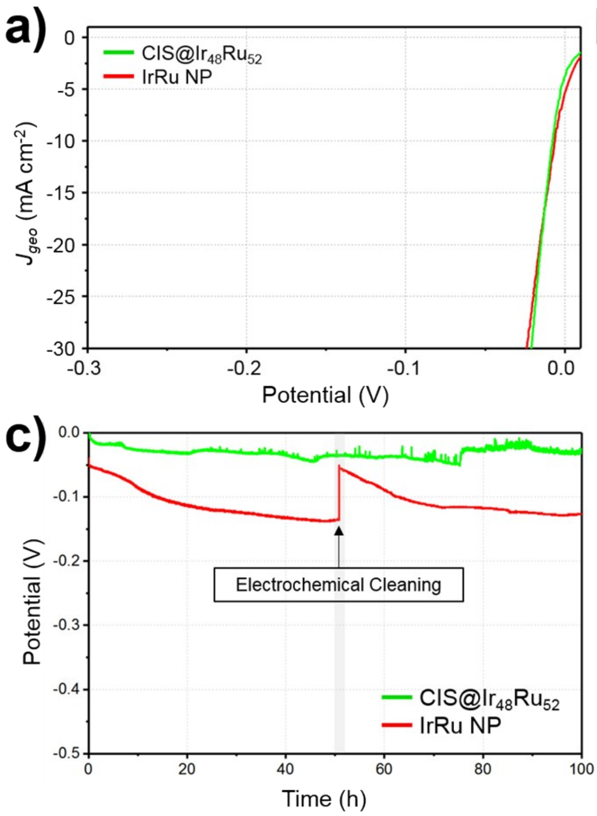

Fig. S22. Comparison of a) HER activity, b) OER activity, and c) HER stability. In c), CIS@$Ir_{48}Ru_{52}$ and IrRu showed constant current density for 100 h of constant reaction. Current drop (red) was due to surface oxidation of metallic IrRu on IrRu NP surface to Ir/Ru oxides. After electrochemical cleaning at 50 h, HER activity was temporally recovered, however the HER activity dropped gradually again.

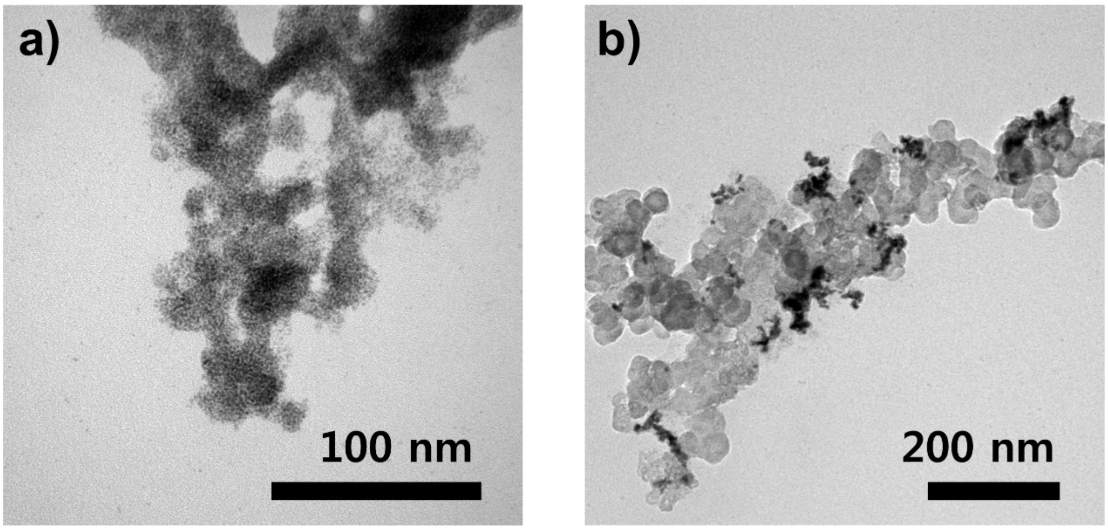

Fig. S23. TEM images of IrRu NPs (a) before and (b) after OER stability test. The IrRu NPs are agglomerated after OER stability test, which might affect the electrocatalytic activity

Supporting Tables S1 to S8.

Catalyst	Ir	Ru	Cu	S
	Atomic %	Atomic %	Atomic %	Atomic %
CIS@Ru	-	54.93	23.74	22.31
CIS@$Ir_{18}Ru_{82}$	7.59	38.62	33.43	20.34
CIS@$IR_{34}Ru_{64}$	12.35	23.99	35.68	27.96
CIS@$Ir_{48}Ru_{52}$	21.55	23.18	31.92	23.33
CIS@$Ir_{67}Ru_{33}$	21.91	10.75	38.63	28.69
CIS@$Ir_{82}Ru_{18}$	32.90	7.02	32.85	27.21
CIS@Ir	37.51	-	30.33	32.14
IrRu NPs	49.52	50.48	-	-

Table S1. Energy dispersive X-ray spectrum (EDS) analysis of cactus like CIS@Ir_xRu_{1-x} with various ratio of Ir to Ru.

Catalyst	Weight on electrode		ECSA	HER			OER		
				Overpotental (mV)		Tafel slope	Overpotental (mV)		Tafel slope
	Ir (μg cm^{-2})	Ru (μg cm^{-2})	m^2 g$^{-1}_{IrRu}$	at 10 mA cm^{-2}	at 20 mA cm^{-2}	mV dec^{-1}	at 10 mA cm^{-2}	at 20 mA cm^{-2}	mV dec^{-1}
CIS@Ru	-	13.7	153.4	101.7	>140	73.0	>500	-	287.2
CIS@Ir$_{18}$Ru$_{82}$	3.4	9.2	143.3	25.4	46.1	35.8	231.3	250.4	51.3
CIS@IR$_{34}$Ru$_{64}$	5.6	5.8	222.5	15.2	24.9	32.2	225.8	244.8	57.6
CIS@Ir$_{48}$Ru$_{52}$	8.5	4.8	78.3	7.6	15.0	25.1	244.4	266.1	57.6
CIS@Ir$_{67}$Ru$_{33}$	9.3	2.4	97.5	12.1	19.8	31.6	266.6	293.5	64.8
CIS@Ir$_{82}$Ru$_{18}$	12.1	1.4	89.1	10.0	15.7	29.8	269.4	297.6	68.4
CIS@Ir	13.5	-	50.5	8.2	14.8	24.2	306.8	330.6	66.7
Pt/C (20%)	12.7 (Pt)	-	93.9 (m^2 g$^{-1}_{Pt}$)	9.4	16.33	23.9	-	-	-
Ir/C (20%)	12.7 (Ir)	-	59.7 (m^2 g$^{-1}_{Ir}$)	15.2	25.8	31.5	311.8	336.7	65.9

Table S2. Table for HER and OER activities of various CIS@Ir$_x$Ru$_{1-x}$, Pt/C and Ir/C.

Reaction	Ru 3d		Ir4f	
	Metallic Ru	Oxidized Ru	Metallic Ir	Oxidized Ir
	Area %	Area %	Area %	Area %
As-synthesized	65.29	34.71	72.81	27.19
After HER	37.66	62.34	60.55	39.45
After OER	34.85	65.15	25.51	74.49

Table S3. Table for XPS peak area of Ru 3d and Ir 4d with before and after electrocatalytic reaction

Catalyst	Overpotential at 10 mA cm^{-2}	Tafel slope mV dec^{-1}	Electrolyte	reference
$CIS@Ir_{48}Ru_{52}$	7.6	25.1	0.1M $HClO_4$	**this work**
Pt/C	9.4	23.9	0.1M $HClO_4$	**this work**
$Cu_7S_4@MoS_2$	133	48	0.5M H_2SO_4	**1**
$MoS_{1.65}$ NCs	60	29	0.5M H_2SO_4	**2**
Rh_2S_3 nanoprism	122	44	0.5M H_2SO_4	**3**
$Cu_{2-x}S@Ru$ nanoplates	129	51	0.5M H_2SO_4	**4**
α-FeNiS	105	40	0.5M H_2SO_4	**5**
β-FeNiS	117	48	0.5M H_2SO_4	**5**
$1T-WS_2$ nanosheets	230	55	0.5M H_2SO_4	**6**
$Pt-MoS_2$	139	96	0.5M H_2SO_4	**6**
Ni_5P_4	24	27	0.5M H_2SO_4	**7**
FeP/CC	34	29.2	0.5M H_2SO_4	**8**
$Fe_{0.5}Co_{0.5}P/CC$	39	30	0.5M H_2SO_4	**9**
Ni_xP_y	40	46.1	0.5M H_2SO_4	**10**
CoP NPs/CC	48	70	0.5M H_2SO_4	**11**
RuNi	41	31	0.5M H_2SO_4	**12**
Ru nanosheets	20	46	0.5M H_2SO_4	**13**

Table S4. Table for HER performances of $CIS@Ir_{48}Ru_{52}$ in this work and other state-of-the-arts catalysts.

Catalyst	**Overpotential at 10 mA cm^{-2}**	**Tafel slope mV dec^{-1}**	**Electrolyte**	**reference**
CIS@$Ir_{48}Ru_{52}$	244.4	57.6	0.1M $HClO_4$	**this work**
CIS@$Ir_{34}Ru_{66}$	225.8	60.3	0.1M $HClO_4$	**this work**
Ir/C	311.8	65.9	0.1M $HClO_4$	**this work**
IrO_x/$SrIrO_3$	270	50	0.5M H_2SO_4	**14**
Co-IrCu ONC/C	293	50	0.1M $HClO_4$	**15**
IrNiCu DNF/C	303	48	0.1M $HClO_4$	**16**
IrNi-RF/C	313.6	48.6	0.1M $HClO_4$	**17**
IrCoNi PHNC/C	303	53.8	0.1M $HClO_4$	**18**
$Cu_{1.11}Ir$	286	43.8	0.05M H_2SO_4	**19**
$Ni_{2.53}Ir$ NC	302	46.6	0.05M H_2SO_4	**20**
3D Ir	270	-	0.1M $HClO_4$	**21**
Ir NPs	340	64	0.1M $HClO_4$	**22**

Table S5. Table for OER performances of CIS@$Ir_{48}Ru_{52}$ in this work and other state-of-the-arts catalysts.

References

1. J. Xu, J. Cui, C. Guo, Z. Zhao, R. Jiang, S. Xu, Z. Zhuang, Y. Huang, L. Wang and Y. Li, *Angew. Chem., Int. Ed.*, 2016, **55**, 6502-6505.
2. L. Lin, N. Miao, Y. Wen, S. Zhang, P. Ghosez, Z. Sun and D. A. Allwood, *ACS Nano*, 2016, **10**, 8929-8937.
3. D. Yoon, B. Seo, J. Lee, K. S. Nam, B. Kim, S. Park, H. Baik, S. Hoon Joo and K. Lee, *Energy Environ. Sci.*, 2016, **9**, 850-856.
4. D. Yoon, J. Lee, B. Seo, B. Kim, H. Baik, S. H. Joo and K. Lee, *Small*, 2017, **13**, 1700052.
5. X. Long, G. Li, Z. Wang, H. Zhu, T. Zhang, S. Xiao, W. Guo and S. Yang, *J. Am. Chem. Soc.*, 2015, **137**, 11900-11903.
6. A. Ambrosi, Z. Sofer and M. Pumera, *Chem. Commun.*, 2015, **51**, 8450-8453.
7. Y. Feng, X.-Y. Yu and U. Paik, *Chem. Commun.*, 2016, **52**, 1633-1636.
8. X. Yang, A.-Y. Lu, Y. Zhu, S. Min, M. N. Hedhili, Y. Han, K.-W. Huang and L.-J. Li, *Nanoscale*, 2015, **7**, 10974-10981.
9. D. Zhou, L. He, W. Zhu, X. Hou, K. Wang, G. Du, C. Zheng, X. Sun and A. M. Asiri, *J. Mater. Chem. A.*, 2016, **4**, 10114-10117.
10. J. Tian, Q. Liu, Y. Liang, Z. Xing, A. M. Asiri and X. Sun, *ACS Appl. Mater. Inter.*, 2014, **6**, 20579-20584.
11. Y. Libin, Q. Honglan, Z. Chengxiao and S. Xuping, *Nanotechnology*, 2016, **27**, 23LT01.
12. C. Zhang, Y. Liu, Y. Chang, Y. Lu, S. Zhao, D. Xu, Z. Dai, M. Han and J. Bao, *ACS Appl. Mater. Inter.*, 2017, **9**, 17326-17336.
13. X. Kong, K. Xu, C. Zhang, J. Dai, S. Norooz Oliaee, L. Li, X. Zeng, C. Wu and Z. Peng, *ACS Catal.*, 2016, **6**, 1487-1492.
14. L. C. Seitz, C. F. Dickens, K. Nishio, Y. Hikita, J. Montoya, A. Doyle, C. Kirk, A. Vojvodic, H. Y. Hwang, J. K. Norskov and T. F. Jaramillo, *Science*, 2016, **353**, 1011-1014.
15. T. Kwon, H. Hwang, Y. J. Sa, J. Park, H. Baik, S. H. Joo and K. Lee, *Adv. Funct. Mater.*, 2017, **27**, 1604688.
16. J. Park, Y. J. Sa, H. Baik, T. Kwon, S. H. Joo and K. Lee, *ACS Nano*, 2017, **11**, 5500-5509.
17. H. Jin, Y. Hong, J. Yoon, A. Oh, N. K. Chaudhari, H. Baik, S. H. Joo and K. Lee, *Nano Energy*, 2017, **42**, 17-25.
18. J. Feng, F. Lv, W. Zhang, P. Li, K. Wang, C. Yang, B. Wang, Y. Yang, J. Zhou, F. Lin, G. C. Wang and S. Guo, *Adv. Mater.*, 2017, **29**, 1703798.
19. C. Wang, Y. Sui, G. Xiao, X. Yang, Y. Wei, G. Zou and B. Zou, *J. Mater. Chem. A.*, 2015, **3**, 19669-19673.
20. C. Wang, Y. Sui, M. Xu, C. Liu, G. Xiao and B. Zou, *ACS Sustainable Chem. Eng.*, 2017, **5**, 9787-9792.
21. Y. Pi, N. Zhang, S. Guo, J. Guo and X. Huang, *Nano Lett.*, 2016, **16**, 4424-4430.
22. T. Reier, M. Oezaslan and P. Strasser, *ACS Catal.*, 2012, **2**, 1765-1772.